mist-jet system includes: 1) inlet, compression and injection losses; 2) inlet drag; 3) expansion of the water particle-air continuum mixture; 4) heat transfer between water particles and air; 5) shattering of water particle during the expansion; 6) wall friction.

This theory agrees with the results of a small experiment as shown in Fig. 1. The experiment consists of a 4-ft expansion nozzle with a 32-in^2 inlet area.

The performance of a 4- × 8-ft inlet area, 100-knot mist jet is shown in Fig. 2. In order to reach optimum efficiency relatively long nozzles are required. Shorter nozzles are possible at only a small sacrifice in efficiency.

A Water-Augmented Air Jet for the Propulsion of High-Speed Marine Vehicles

ROLF K. MUENCH* AND ALLEN E. FORD†
Naval Ship Research and Development Laboratory, Annapolis, Md.

An analysis along with results of a small-scale, static experiment are presented. The analysis includes the effect of momentum transfer between the air and the water particles, the shattering of the particles exposed to an air stream, losses attributed to heat transfer between the air and the water, wall friction, etc. The experimental thrust data are shown to agree with the theoretical predictions over the entire range of water-air mass flow tested. The performance of this propulsion system is examined as a function of ship speed, nozzle length, etc.

Nomenclature

A = two-phase nozzle cross-sectional area
A_s = water inlet cross-sectional area
C = liquid-phase specific heat
C_p = gas-phase specific heat
C_D = particle drag coefficient
C_{DS} = inlet drag coefficient
D = particle diameter
D_H = hydraulic diameter
D_S = inlet drag
F_D = particle drag force
h = heat-transfer coefficient
H_i = initial nozzle heights
K = freestream dynamic pressure recovery coefficient
L = nozzle length
$\dot{m}$ = mass flow rate
Nu = Nusselt number
P = static pressure
r = mass flow ratio
R = gas constant
Re = Reynolds number
q = particle heat transfer
S = two-phase nozzle slope
$\hat{T}$ = characteristic particle shattering time
$\hat{T}_H$ = characteristic particle shattering time according to Haas[13]
T = temperature
T_i = initial or ambient temperature
V = velocity
w = two-phase nozzle width
We = Weber number
X = two-phase nozzle coordinate
γ = ratio of specific heats
η_c = compressor efficiency
η_0 = propulsion efficiency
ν = stagnation pressure ratio
ρ = density
σ = liquid-gas velocity ratio
θ = thrust
τ_w = two-phase wall shear

Subscripts

Ex = exit condition
g = gas phase
ℓ = liquid phase
S = ship condition

Presented as Paper 69-405 at the AIAA 2nd Advanced Marine Vehicles and Propulsion Meeting, Seattle, Wash., May 21–23, 1969; submitted May 15, 1970; revision received July 27, 1970.

* Mechanical Engineer, Power and Propulsion Division. Associate Member AIAA.
† Mechanical Engineer, Power and Propulsion Division.

Introduction

THE water-augmented air jet or mist jet is a reliable, lightweight, high-speed marine propulsion system, utilizing a two-phase propulsion fluid. That is, a mixture of water and air, both of which are plentiful at the ocean surface, is expanded through a nozzle to produce thrust. The process is properly referred to as augmentation since the air jet is capable of producing thrust by itself.

The concept of two-phase propulsion is not new in the marine propulsion field. Past efforts have primarily been centered on the hydroramjet,[1] its pulse-jet cousin, and the liquid ejector using either compressed air or steam.[2] In general, these systems suffer from high heat-transfer losses to the water, since they use either adiabatically compressed high-pressure air or combustion products. Others fail to provide zero velocity thrust and thus require auxiliary propulsion power plants.

The water-augmented air jet is a more recent addition to the two-phase marine-propulsion field. It represents an improvement over the other systems since it is partially able to overcome some of their problems, such as excessive heat-transfer losses and the lack of static thrust. Preliminary studies of this concept were published by Muench and Keith[3] and Davison and Sadowski.[4]

It has been mentioned that the mist jet is a lightweight system. This is basically a result of eliminating mechanical transmission elements and using aircraft-type power plants. This system employs a turbofan which is usually designed for subsonic speed (500 knots). By injecting water in the form of particles into the bypass air, the system is suited for propulsion of prospective high-speed marine vehicles. The turbofan and associated equipment for injecting water and the two-phase expansion nozzle are still light compared to the water jet and super-cavitating propeller. The bypass air of the turbofan, with a pressure ratio between 1.3 and 1.5, is especially suited, since the efficiency of the mist jet decreases

with increasing pressure ratio and the size of the system increases appreciably below a compression ratio of 1.3. The decrease in efficiency at higher-pressure ratios is primarily due to heat-transfer losses from the air to the water and larger spray losses associated with higher air pressures.

A typical high-speed ship installation of the mist jet is shown in Fig. 1. In order to avoid salt spray and water ingestion, the turbofan inlet should be located high above the water line. Lifting the water to the fan exhaust will result in an appreciable loss in spray pressure; therefore, the spray station is located near the water line and the air is ducted down. The purpose of the spray station is to inject water in the form of small droplets coaxially with the air stream. The mixture of air and water is then expanded to ambient pressure.

In the system shown in Fig. 1, the spray pressure is equal to the portion of the freestream stagnation pressure recovered by the high-speed inlet, less the water lift and other losses. At low ship speeds insufficient pressure is available to establish water flow against the air pressure at the spray station. A pump can be installed to boost the spray pressure, but it should be pointed out that the addition of a pump to handle the high water mass flow sacrifices the basically simple and lightweight features of the propulsion system. Relying on the inlet recovery to provide the spray pressure requires that sufficient unaugmented thrust is available to accelerate the ship to the speed where augmentation is possible.

The thrust augmentation is due to the increased mass flow at constant power input, which decreases the exit velocity resulting in lower kinetic energy losses to the wake. This augmentation in thrust by lowering the wake loss is not accomplished without increasing the losses in other areas. For instance, water has to be brought onboard, requiring high-speed water inlets that introduce some additional drag and some recovery pressure that is less than the stagnation pressure. One might wonder if these additional considerations do not outweight the gain. Therefore it was necessary for the analysis outlined in the next section to include reasonable values for all major losses.

It should be mentioned that as the system evolved it was realized that comparison with other possible high-speed propulsion systems (supercavitating propellers and water jets) could not be based on efficiency alone. The mist jet, although lighter and cheaper, unfortunately is less efficient than the other systems mentioned previously. It is therefore more meaningful to compare the propulsion system performance on an over all or economic basis, accounting for the payload, fuel consumption, initial cost, etc. Smith and Fox,[5] and more recently Garrett and Quandt,[6] published an economic analysis of small captured-air-bubble ships powered by mist jets, water jets, and supercavitating propellers. They found that the lighter weight, lower-cost mist jet can overcome its efficiency handicap at speeds in excess of 75 knots.

Analysis

Although it was stated in the previous section that the efficiency alone is not sufficient to judge the performance of the mist jet, this paper will describe the system strictly in terms of net thrust and/or efficiency. It will be seen that the proper calculation of these two parameters is necessary to carry out further system optimization.

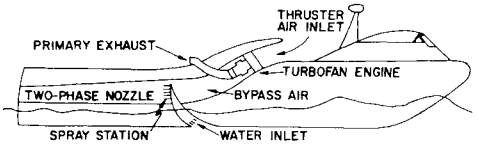

Fig. 1 Schematic of mist-jet installation in high-speed ship.

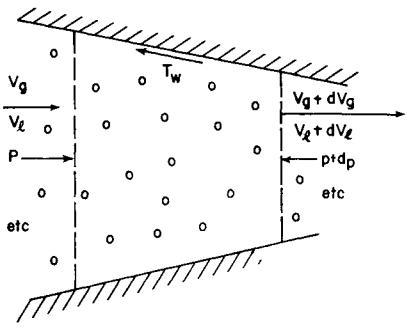

Fig. 2 Control volume for total flow considerations.

The definition of the net thrust for a two-phase flow is

$$\theta = \dot{m}_g(V_{gEx} - V_S) + \dot{m}_\ell(V_{\ell Ex} - V_s) - D_S = \dot{m}_g[V_{gEx} + rV_{\ell Ex} - (1 + r)V_S] - C_{DS}\tfrac{1}{2}\rho_\ell V_S^2 A_S \quad (1)$$

where, in general, the exit velocity of the two phases are not equal. The efficiency is now defined as the net thrust power divided by the shaft power into the compressor.

$$\eta_0 = \frac{\theta V_S \eta_c}{\dot{m}_g C_p T^0{}_i \{\nu^{[(\gamma-1)/\gamma]} - 1\}} = \frac{V_{gEx} + rV_{\ell Ex} - (1 + r)V_S - \tfrac{1}{2}rC_{DS}\, V_S A_S/A_0}{C_p T_i{}^0 \{\nu^{[(\gamma-1)/\gamma]} - 1\}} \quad (2)$$

Because of the reference to shaft power input, this definition is not clearly appropriate when considering turbofan engines for the mist jet, but it is convenient when comparing results with shaft powered units.

The efficiency is a function of the nozzle exit velocity of the two phases and the mixture ratio. The velocities can easily be calculated by assuming that they are equal or the liquid velocity is a given fraction of gas velocity. This is not very realistic since it does not properly include the losses attributed to two-phase flow, nor will it yield any information on optimum nozzle length or shapes. Elliot,[7] and more recently Elliot and Weinberg,[8] have shown that a two-phase liquid-particle gas-continuum flow can be analyzed quite accurately with the following considerations: 1) The phases can be treated separately. 2) The liquid phase consists of uniform spherical particles. 3) The particles are accelerated by aerodynamic forces. 4) The particles shatter in accordance with the Weber criterion.

From these considerations a one dimensional conservation equation for each of the two separate phases and the total flow can be written, with only two of the three being independent. The total continuity equation can be written for the control volume as shown in Fig. 2.

$$A = A_g + A_\ell = (\dot{m}_g/\rho_g V_g) + (\dot{m}_\ell/\rho_\ell V_\ell) = (\dot{m}_g/\rho_g V_g)[1 + (r/\sigma)(\rho_g/\rho_\ell)] \quad (3)$$

Since the continuity equation for each phase is $\dot{m}_g = \rho_g A_g V_g$ and $\dot{m}_\ell = \rho_\ell A_\ell V_\ell$.

Similarly, the total momentum equation can be written for the control volume shown in Fig. 2.

$$\dot{m}_g(dV_g/dX) + \dot{m}_\ell(dV_\ell/dX) = -A(dp/dX)\pi D_H \tau_w \quad (4)$$

That is, the sum of the momentum changes of the two phases is equal to the forces (pressure and viscous) on the control volume. For the momentum equation of the water particles, it is more convenient to use the particle surface as the boundary of the control volume (Fig. 3). The force on the control volume is equal to the mass times acceleration of the particle. Neglecting the buoyancy force, the momentum equation for the particle can be written as

$$F_D = \frac{\pi D^3}{6}\rho_\ell \frac{dV_\ell}{dX_\ell} V_\ell = C_D \frac{\pi D^2}{4}\frac{1}{2}\rho_g(V_g - V_\ell)\,|V_g - V_\ell|$$

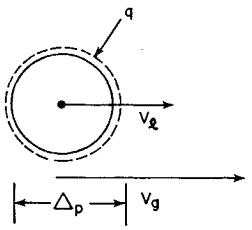

Fig. 3 Control volume for a single particle.

which can be simplified as follows:

$$dV\ell/dX = \tfrac{3}{4}(C_D/D)(\rho_g/\rho_\ell)[(V_g/V_\ell) - 1]|(V_g/V_\ell) - 1|V_\ell \quad (5)$$

Assuming that the heat transfer between the wall and two-phase flow is negligible, the total energy equation can be written in the following form:

$$\dot{m}_g[C_p dT_g + (dV_g^2/2)] + \dot{m}_\ell[CdT_\ell + (dp/\rho_\ell) + (dV_\ell^2/2)] = 0 \quad (6)$$

For the particle energy equation, it is convenient to use the control volume shown in Fig. 3. The heat transfer to a single particle considering conduction only is $q = h\pi D^2(T_g - T_\ell)$. The heat transfer to all the particles crossing a given station in the nozzle per unit time is equal to the rate of change of the internal energy of this cloud of particles, or

$$C\dot{m}_\ell(dT_\ell/dt) = C\dot{m}_\ell V_\ell(dT_\ell/dX) = (6\dot{m}_\ell/\pi D\rho_\ell)\pi D^2 h(T_g - T_\ell)$$

Simplifying this equation,

$$dT_\ell/dX = 6/D(h/C\rho_\ell V_\ell)(T_g - T_\ell) \quad (7)$$

It should be mentioned that for the gas phase, the perfect gas equation of state is used.

$$p = \rho_g R_g T_g \quad (8)$$

The aforementioned six equations [Eqs. (3–8)] for the two-phase nozzle flow contain 7 unknowns (V_ℓ, V_g, A, T_ℓ, T_g, ρ_g, and p) as a function of the longitudinal nozzle coordinate X. One additional specification is needed to complete the set and find the solution. One might specify that the resulting nozzle configuration have maximum thrust for a given length, but this is a variational problem, the solution of which is difficult to obtain. If on the other hand the nozzle profile is specified as a function of longitudinal nozzle coordinate in the following form:

$$A = W(H_i + SX + \ldots \quad (9)$$

a solution can easily be found with the help of a digital computer. An optimum solution of these equations is possible only by examining a large number of nozzle profiles.

The results shown in this report were calculated with the air of an IBM 360 Model 40 computer using the Runge-Kutta method as modified by Mason.[9] The equations are integrated as a function of the longitudinal nozzle coordinates until the ambient pressure is reached. The exit velocities are then used to calculate the thrust or efficiency with the aid of Eq. (1) or (2).

In the integration of the conservation equations additional information is needed for the particle drag coefficients, heat-transfer coefficient, and two-phase wall friction. For the particle-drag coefficient, the following set of equations was used:

$$C_D = 24/Re, \quad Re \leq 0.1 \quad (10a)$$

$$\ln C_D = 3.271 - 0.8893 \ln Re + 0.03417(\ln Re)^2 + 0.001443(\ln Re)^3, \quad 0.1 < Re < 2 \times 10^4 \quad (10b)$$

The first equation is known as the Stokes law, and the second is a least square fit, by Stonecypher,[10] to experimental solid-sphere drag-coefficient data. Reynolds numbers in excess of 2×10^4 are never encountered in this particular problem. The heat-transfer coefficient was calculated from a semi-empirical relation from Drake.[11]

$$Nu = 2.0 + 0.40Re^{0.55}, \quad Re < 2.0 \times 10^5 \quad (11)$$

The two-phase wall friction is calculated with the aid of a simple modification of the familiar Blasius equation, by substituting mass average two-phase properties for all parameters except the Reynolds number. The modified Blasius equation then takes on the following form:

$$\tau_w = 0.0288\rho_g V_g^2 \frac{1 + r/\sigma}{1 + r/\sigma\ \rho_g/\rho_\ell}\left(\frac{1 + r\sigma}{1 + r}\right)^2 Re^{-1/5} \quad (12)$$

It is important to include the wall friction, since a typical mist-jet nozzle will measure more than 10 ft in length.

When the Weber number of the water particle exceeds the critical value (6.0), it is well known that the particle will shatter. Unfortunately, very limited information on the rate at which the particles shatter and their resulting particle size is available. This is the reason investigators (Elliot,[7] Elliot and Weinberg,[8] and Davison and Sadowski[4]) so far have assumed that the particle diameter is in equilibrium with the critical Weber number. In this analysis, it is assumed that the particles shatter at a rate given by the following rate equation:

$$(d/dt)(D - D|_{We=6}) = (1/\hat{T})(D - D|_{We=6})$$

where $\hat{T}$ is a characteristic time. This equation can be integrated, and the constant of integration can be evaluated with the initial condition $D = D_i$.

$$D - D|_{We=6} = (D_i - D|_{We=6})e^{t/\hat{T}} \quad (13)$$

A characteristic time ($\hat{T}$) that is equal to the natural period of the particle as suggested by Morrell[12] has been used.

$$\hat{T} = (1/2\pi)[(D^2/64)(\rho_\ell/\rho_g)]^{1/3} \quad (14)$$

Furthermore, a characteristic time based on the experimental shattering results of Haas.[13]

$$\hat{T}_H = 2 \times 10^{-3} \text{ sec} + 1.75(D/V_g - V_\ell)(\rho_\ell/\rho_g)^{1/2} \quad (15)$$

also was tried. As will be seen in the next section, the results using Eq. (14) or (15) are not significantly different.

This summarizes the analysis of nozzle expansion, except for the nozzle inlet conditions. The inlet conditions are a function of the water inlet performance, pressure losses of the water and air ducting, turbofan performance, ship velocity, etc. These considerations are straightforward and are fully detailed elsewhere.[3,14]

Experiment

To increase the confidence level of the theoretical model of the mist jet presented previously and to establish the seriousness of anticipated and unanticipated problem areas, a small static model was designed and tested.[15] Figure 4 shows the

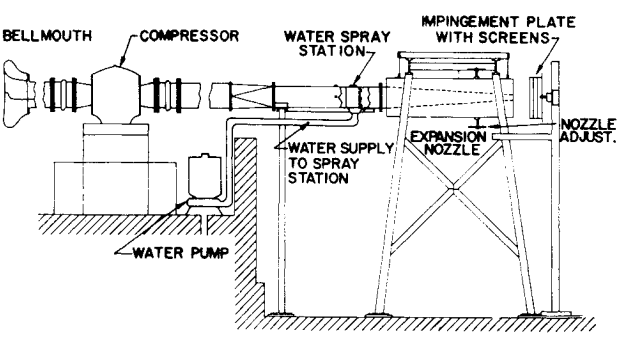

Fig. 4 Schematic of mist-jet experiment.

schematic of the experimental system. The compressor for the air supply, the pump for the water supply, the instrumentation readouts, and the electrical control panel are located inside the building. The spray station, two-phase nozzle, and impingement plate for the measurement of static thrust are located outside the building, for obvious reasons. To minimize the thrust error because of water splashing, progressively larger wire screens were fastened on the front of the impingement plate. Figure 5 shows an external view of the experimental in operation, but without the impingement plate installed.

Just upstream of the impingement plate is the 4-ft-long, two-phase nozzle with an inlet cross section, 4 in. wide and 8 in. high. The exit area can be adjusted with the movable top and bottom walls. The spray station is located upstream of the two-phase nozzle. During the experimental program, three different spray station configurations were tested.

The first spray station consisted of an 8-in.-high wedge with a sharp leading edge and a $1\frac{3}{4}$-in.-wide trailing edge, on which were fastened up to 11 spray nozzles facing downstream. This rather simple spray station introduces a pressure loss and turbulence to the gas phase. Furthermore, the spray nozzles were concentrated near the centerline of the duct, resulting in a nonuniform particle distribution at the two-phase nozzle inlet. A second spray station was therefore designed and built to provide a more uniform nozzle inlet particle distribution and to minimize the disturbance to the air phase. This spray station configuration consists of four 8-in.-long spray struts with a total of 38 spray nozzles. An attempt was also made to streamline the spray nozzles and struts to minimize gas-phase pressure loss and turbulence. Experimental data from these two spray station configurations show the same relationship to the theory as shown in Figs. 6 and 7. Therefore, it can be concluded that the higher turbulence associated with the first spray station is as effective in generating a uniform particle distribution as the mechanical distribution of the second spray station. It was necessary to compare the data with the theory rather than compare the data of the two spray stations directly, since they have different water flow capacities.

In order to collect some data that might be typical of an actual ship installation, a third spray station with large nozzles was fabricated and tested. Due to size limitation of this experiment, the spray station consists of only 4 spray nozzles (spraying system $1\frac{1}{4}$ U 151000 Vee Jet nozzles) positioned on a single-center strut. Unfortunately, the results from this spray station did not correlate with the theoretical results. It was noticed that these large nozzles have a long undisturbed jet before particles begin to form. It is suspected that the short nozzle used with the present experimental was sensitive to this phenomenon.

Figures 6 and 7 show the theoretical thrust based on both the natural-period shattering rate and the breakup rate due to Haas[13] (experimental). There is a slight difference between the two shattering rates, with the natural-period shattering rate agreeing better with the data. Assuming a shattering rate that is equal to twice or ten times the natural-period results in a much poorer prediction (Fig. 6).

The unaugmented thrust or zero augmentation limit shown along with the data and theory in Figs. 6 and 7 is based on the premise that no interaction between air and water takes place during the air expansion through the nozzle, that is, the water

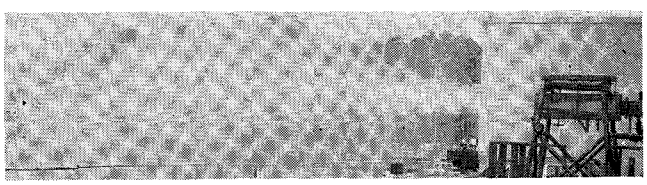

Fig. 5 External view of the mist-jet experiment in operation without impingement plate.

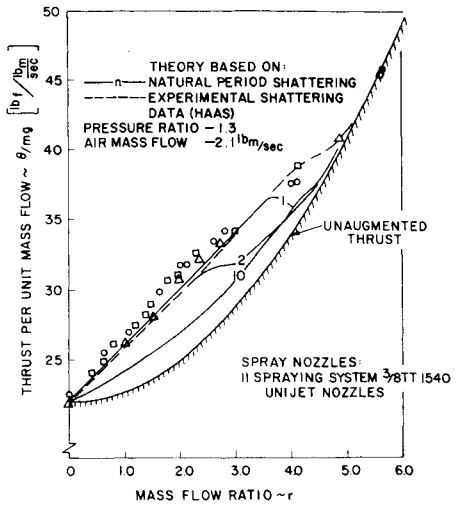

Fig. 6 Experimental and analytical results for first spray station configuration.

exit velocity is equal to the injection velocity and the air exit velocity is fixed by the pressure ratio (ν). At low values of the mixture ratio (r) the experimental results and theory are well above the unaugmented limit, but at high mixture ratio both theory and experiment approach this limit.

Examining the theoretical particle history in the nozzle, one finds that at high mixture ratios the average particle size is much larger than at lower mixture ratios. This is a consequence of the constant spray nozzle area, where the only way the mixture ratio can be changed is to change the water-supply pressure and in turn the water-injection velocity. Thus, a low mixture ratio corresponds to a low water velocity, but a high Weber number ($We \sim V_g - V_\ell$) means rapid shattering of the particles and relatively efficient acceleration of the particles. As the mixture ratio increases, the water velocity approaches the air velocity and no shattering and little acceleration of the particles will occur. The minimum theoretical particle sizes for different spray stations can then

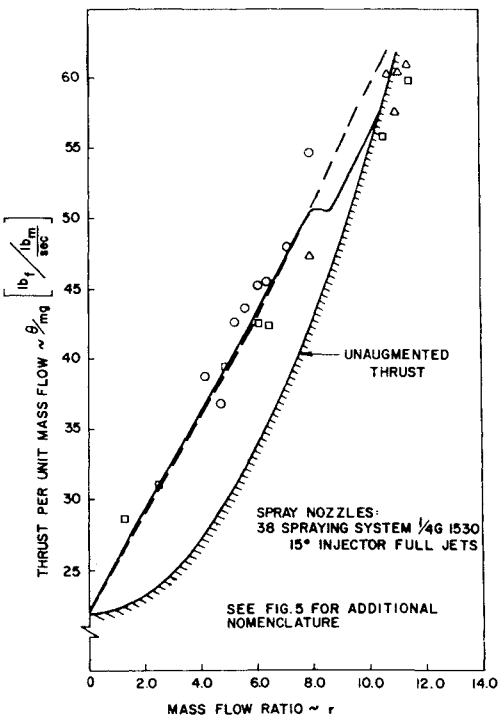

Fig. 7 Experimental and analytical results for second spray station configuration.

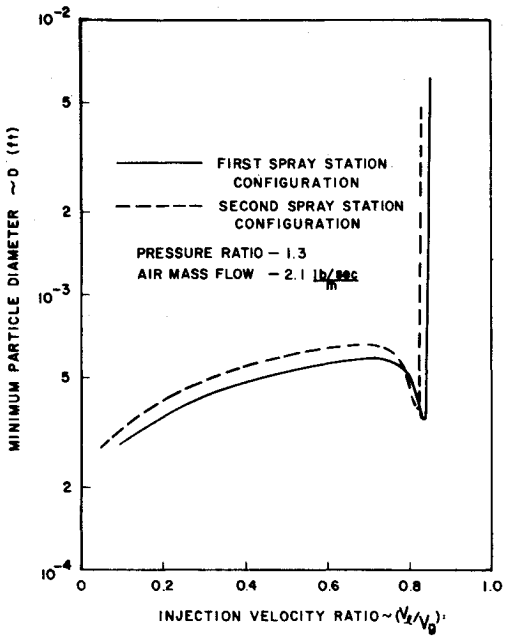

Fig. 8 Minimum theoretical particle diameter.

be united by plotting them as a function of the injection velocity rato ($\sigma = V_\ell/V_g$) (Fig. 8). It can be seen from this figure that in the design of mist-jet propulsion systems, an initial slip of less than 0.8 should be employed.

The thrust of the propulsion system is equal to the propulsion-fluid momentum change across the system. In a ship installation this can be separated into the gross thrust and ram drag. The gross thrust is equal to the exit velocity times the mass flow and the ram drag is equal to the ship velocity times the mass flow. Since the thrust measured by the impingement plate is equal to the gross thrust, an actual ship installation would produce a thrust which is less than the experimental thrust by the amount of the ram drag. Therefore, the augmentation ratio of a ship installation is more than the 25% shown in Figs. 6 and 7.

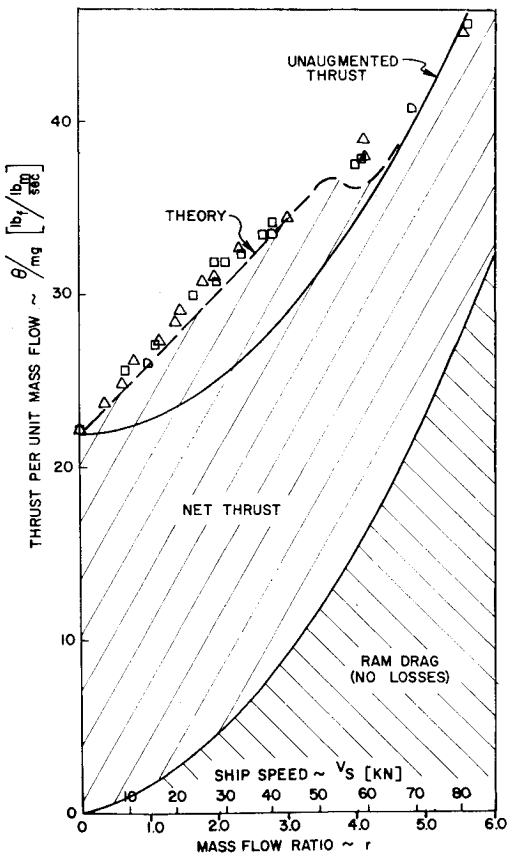

Fig. 9 Static test-ship comparison.

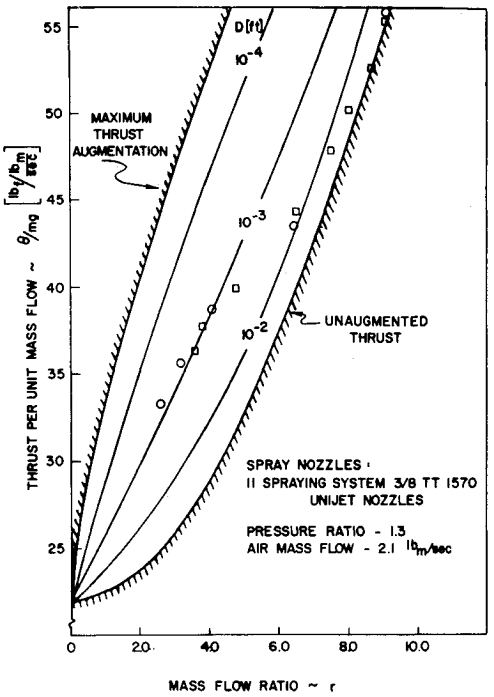

Fig. 10 Experimental and constant particle analytical results for second spray station configuration.

The ram drag, which is a function of the ship speed, can be related to the mass flow ratio of the experiment with the aid of the following equation:

$$r = \dot{m}_\ell/\dot{m}_g \cong \rho_\ell V_{\ell i} A_n/\dot{m}_g = \rho_\ell V_S A_n/\dot{m}_g$$

where A_n is the total nozzle area of a given spray station, and it has been assumed that no losses are encountered by the water, or the water injection velocity ($V_{\ell i}$) is equal to the ship speed (V_s). The data from Fig. 5 have been replotted as a function of ship speed in Fig. 9. Also shown in this figure is the ram drag in relation to the experimental data. The net thrust now shows an augmentation of more than 40% at 40 knots. It should be pointed out that the point of maximum thrust or maximum efficiency can be designed to occur at any desired ship speed.

At a pressure ratio of 1.3 the augmentation is not limited to 25%, but up to 80% augmentation of the gross thrust can be realized if the exit velocities of the two phases are equal (maximum augmentation). Figure 10 shows experimental results from the first spray station with larger spray nozzles than used in Fig. 6. Also shown are theoretical results based on constant particle size, zero, and maximum augmentation. The equal exit velocities needed for maximum augmentation are only possible with infinitesimally small water particles. For small values of the mixture ratio, the data parallel the theory based on a constant particle size of 10^{-3} ft. An order of magnitude decrease in particle size results in another 20% increase in augmentation, but it should be remembered that this represents an extremely small particle size. For example, stable fog requires a particle size at only 10^{-4}-ft diam.

Application

Now that some confidence in the analysis has been established, it will be of interest to examine more general mist-jet performance results. It can be anticipated that the efficiency

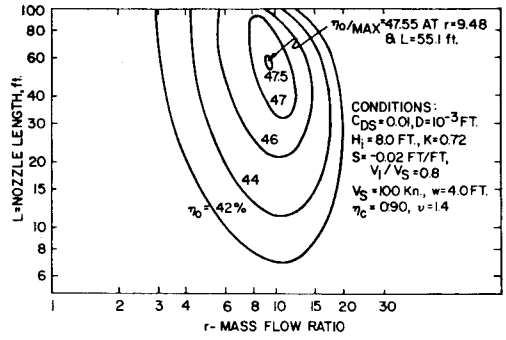

Fig. 11 Efficiency map.

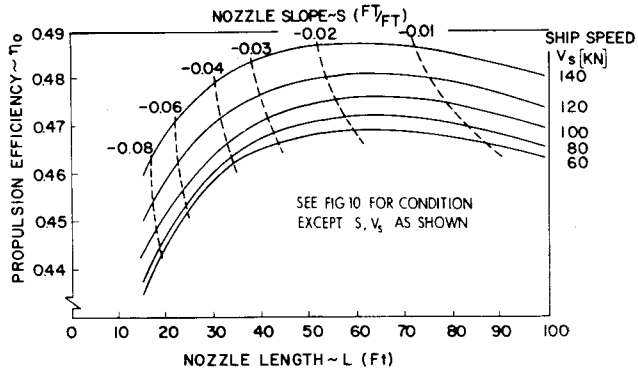

Fig. 12 Theoretical mist-jet efficiency.

is a function of the nozzle parameters, mass flow ratio and ship speed. The efficiency map shown in Fig. 11 demonstrates the effect of the mass flow ratio and nozzle length on the efficiency. It demonstrates the penalty paid by long high mass flow ratio nozzles because of the frictional losses. The decrease in efficiency is very rapid in this area. On the other hand, the relatively smaller decrease in efficiency of short, low mass flow ratio nozzles is due to incomplete acceleration of the particles.

Examination of nozzle slope, or the more significant nozzle length, in relation to efficiency shows that the maximum efficiency occurs at a very large nozzle length (Fig. 12). There is no available configuration that will maintain efficiency with a shorter nozzle. Also shown in Fig. 12 is the effect of ship velocity on the efficiency. Velocities above 100 knots show a more rapid increase in efficiency if all other parameters could be maintained constant. At some higher velocity, this gain is outpaced by the water system losses and therefore a speed for optimum efficiency exists which is primarily a function of the compression ratio and system losses.

It has been stated previously that the mist jet is a simple, lightweight and reliable propulsion system. This implies that water pumps should not be employed to boost the water pressure at the spray station. The addition of these units would increase the weight and decrease the simplicity and reliability of the system. The water induction system would therefore have to rely on the dynamic pressure recovery of the high-speed water inlet. Spraying and augmentation could not commence until the water pressure at the spray station surpasses the air static pressure. For a pressure ratio of 1.4, augmentation would not commence until 17.4 knots.

High-speed marine vehicles such as planning boats and hydrofoils have a high-drag hump at low speed due to wave making or takeoff considerations. Augmentation commences at about the same speed as this drag hump, and thus, sufficient air-only thrust must be available to pass this high point on the drag curve.

This is easily accomplished by installing enough power to negotiate the hump with sufficient margin and then cruise at partial throttle for maximum range. The high-pressure ratio gas turbines used with most turbofan engines have a relatively flat fuel consumption above 50% of maximum power, so this procedure would not cause a marked loss in fuel economy at intermediate speeds.

Concluding Remarks

The experiment demonstrates that thrust augmentation of low-pressure air jets by the injection of water particles is feasible. Furthermore, the resulting two-phase phenomena in the expansion nozzle can be analyzed and predictions of the performance can be calculated with the aid of digital computers. Even though the first experimental program was rather small in scale, it is expected that the analytical-experimental agreement will exist even for large experimental systems.

Studies of potential high-speed ship applications indicate that propulsive efficiencies up to 50% at a ship velocity of 100 knots, a mixture ratio of 10 and a nozzle length of 50 ft are possible. Shorter nozzles are possible at slight decrease in efficiency, but even 50-ft nozzles are not excessive for the very large planform captured-air-bubble ships. The mist jet can overcome the high hump drag without auxiliary propulsion systems, if sufficient power is installed. The lightweight turbofan with its takeoff power and high cycle pressure ratio allows excess power installation without increasing the total weight of the system or the fuel consumption significantly.

References

[1] Anderson, R. G., Rush, G. W., Jr., and McClellan, T. R., "Development of a Hydroduct," thesis, 1947, Guggenheim Aeronautical Lab., California Institute of Technology.

[2] Gouse, S. W. et al., "Heat, Mass and Momentum Transfer in a Condensing Ejector Mixing Section," AIAA Paper 67-420, Washington, D.C., 1967.

[3] Muench, R. K. and Keith, T. G., Jr., "A Preliminary Parametric Study of a Water-Augmented Air-Jet for High Speed Ship Propulsion," MEL R&D Rept. 358-66, Feb. 1966, Marine Engineering Laboratory, Annapolis, Md.

[4] Davison, W. R. and Sadowski, T. J., "Water-Augmented Turbofan Engine," *Journal of Hydronautics*, Vol. 2, No. 1, Jan. 1968, pp. 14–20.

[5] Smith, J. and Fox, R. M., "Reference Design Study of Mist-Jet Propulsion Systems in Captured-Air-Bubble Ships," R&D Rept. 2496, Nov. 1967, Naval Ship Research and Development Center, Annapolis, Md.

[6] Garrett, J. H. and Quandt, E. R., Jr., "Potential Propulsion Systems and Their Effect on the Economics of High Speed Captured-Air-Bubble Craft," presented at the International Marine and Shipping Conference, June 1969, London, England.

[7] Elliot, D. G., "Analysis of the Acceleration of Lithium in a Two-Phase Nozzle," *Proceedings of the 1963 High Temperature Liquid Metals Heat Transfer Technology Meeting*, Dec. 1964, pp. 353–370.

[8] Elliot, D. G. and Weinberg, E., "Acceleration of Liquids in Two-Phase Nozzles," TR 32-987, July 1968, Jet Propulsion Lab.

[9] Mason, T. W., "RKUTTA (Runge-Kutta) CNA Computer Program 21-65S," Contribution No. 12, June 1966, Center for Naval Analysis.

[10] Stonecypher, T. E., "Dynamic and Thermal Non-Equilibrium in Two-Phase Flow in Rocket Nozzles," Rept. P-60-17, Dec. 1960, Rohm and Haas Co.

[11] Drake, R. M., Jr., "Discussion of Forced Convection Heat Transfer from an Isothermal Sphere to Water," *Transactions of the ASME, Ser. C: Journal of Heat Transfer*, Vol. 83, No. 1, pp. 170–172.

[12] Morrel, G., "Critical Conditions for Drop and Jet Shattering," TND-677, Feb. 1961, NASA.

[13] Haas, F. C., "Stability of Droplets Suddenly Exposed to a High Velocity Gas Stream," *Journal of American Institute of Chemical Engineers*, Vol. 10, Nov. 1964, pp. 920–924.

[14] Muench, R. K., "Analysis of the Two-Phase Expansion of a Water-Augmented Air-Jet (U)," Rept. MACHLAB 115, Oct. 1969, Naval Ship Research and Development Lab., Annapolis, Md.

[15] Muench, R. K. and Ford, A. E., "Experimental Results of a Small Water-Augmented Air-Jet," Rept. MACHLAB 116, Oct. 1969, Naval Ship Research and Development Lab., Annapolis, Md.